Far Ultraviolet Electric Linear Dichroism. II. Pulsed Electric Dichroism Apparatus and Dichroic Spectra of Collagen in Aqueous Solution in the 230—187 nm Wavelength Region

Kiwamu YAMAOKA,* Manabu ASATO, Koichiro MATSUDA, and Kazuyoshi UEDA
Faculty of Science, Hiroshima University, Higashisenda-machi, Naka-ku, Hiroshima 730
(Received January 17, 1984)

A Pulsed electric linear dichroism (ELD) apparatus is described for studying the optical properties and solution conformation of biologically important macromolecules whose chromophores absorb light in the far ultraviolet region. This apparatus is capable of generating a rectangular-wave electric pulse field with a duration of 5 μs—5 ms and an amplitude of 0.2—8 kV over the 360—185 nm region. A special feature to this apparatus is its ability to record both parallel and perpendicular dichroism signals simultaneously and independently. To prove the instrumental performance, some dichroic spectra of calfskin collagen solution (pH 3.16 and concentration 0.03 g dm^{-3}) in 0.001 mol dm^{-3} H_3PO_4 were measured in the 230—187 nm region, where the peptide chromophore shows a broad absorption spectrum. The reduced dichroism of collagen was positive but not constant throughout the wavelength region. A detailed analysis revealed that the peptide spectrum contains three overlapping absorption bands centered at 219, 200, and 189 nm. These transition moments were found to be inclined at ±(50.6—51.0°) (219 nm), ±(48.8—49.5°) (200 nm), and ±(56.0—55.8°) (189 nm) relative to the orientation axis of a triple-stranded collagen helix.

When a homogeneous electric field is externally applied to a macromolecular solution, the solute molecules tend to orient toward the direction of the electric field. If these molecules contain chromophoric groups, they absorb linearly-polarized light selectively. The difference in absorbances $\Delta A(=A_{/\!/}^{E}-A_{\perp}^{E})$ between the light component polarized parallel ($A_{/\!/}^{E}$) and perpendicular ($A_{\perp}^{E}$) to the direction of the electric field is a negative or positive quantity, which is termed the electric linear dichroism (ELD).[1-3] By examining the wavelength dependence of reduced dichroism, $\Delta A/A$, inside an absorption band, where A is the isotropic absorbance in the absence of electric field, useful information may be extracted on the relative arrangement between a particular chromophore and the polymer backbone chain and on the overall polymer conformation in solution.

Although natural and synthetic polymers often contain characteristic chromophores in the ultraviolet and far ultraviolet regions, the dependence of $\Delta A/A$ on wavelength has been studied only in a few cases.[1-13] (Related subjects have been reviewed prior to 1973 in Refs. 1—5.) This is mostly because technical difficulties are involved in measuring the electric dichroism spectra; for instance, no commercial instruments are available as yet. The instrumentation of electric dichroism in the visible and near ultraviolet regions has been reported with particular emphasis on a fast and high-voltage square-wave pulse, a widely covered wavelength region, and a high spectral resolution.[6,14] With such a pulsed electric field, the transient dichroic signal of an ionic solution can be measured. This in turn makes it possible to determine the relaxation time and to estimate the overall macromolecular shape.

Such vital biopolymers as nucleic acids, polypeptides, proteins, and polysaccharides all have intrinsic chromophores in the far ultraviolet region. Hence, for the purpose of clarifying the optical properties and solution conformation of these biopolymers, we initiated a series of the far ultraviolet ELD studies. In this paper, we will briefly describe a new ELD apparatus, which can cover 360—185 nm and allow an independent and simultaneous detection of both parallel and perpendicular signals. This procedure is essential to detect any anomalous electrochromic effect,[15] although it has been often ignored. With this apparatus, we will demonstrate some important features associated with ELD spectra of collagen in an acid solution, together with an analytical procedure for observed data.

Apparatus and Data Analysis

Apparatus. A transient ELD apparatus consists of four major parts; the electric, optical, signal-detecting, and measuring-cell systems. The principles and design procedure for such an apparatus have been discussed elsewhere.[1,2,6,14] A new feature was added to the present far ultraviolet ELD apparatus, in such a way that both parallel and perpendcular signals can be recorded by applying a single high-voltage pulse to a sample cell. Figure 1 shows the block diagram of this apparatus. The electric system is unchanged from that previously described in detail.[14] It consists of a pulse generator, a homemade pulse amplifier, a 10 kV DC high-voltage power supply, and a homemade high-voltage pulse discharge network. The single square-wave pulse applied to a measuring "Kerr" cell was attenuated with a Tektronix 1000:1 P6013A probe and fed to a 7A18 plug-in amplifier of a Sony-Tektronix 7844 dual beam oscilloscope. The rise and decay times of a high voltage pulse were confirmed to be less than 1 μs under optimum conditions.[14]

Figure 2 shows the optical system schematically; this was newly designed and constructed for the present purpose. The light source is a water-cooled 200 watt deuterium discharge arc lamp D_2 (D-200F, Original Hanau, West Germany) operated on a 100 volt DC power in the 400—185 nm region. This lamp is about four times as intense as the conventional 40—30 watt deuterium lamp. The monochromatic light from a 25 cm grating double monochromator with low stray light and high wavelength accuracy (0.1 nm) (Japan

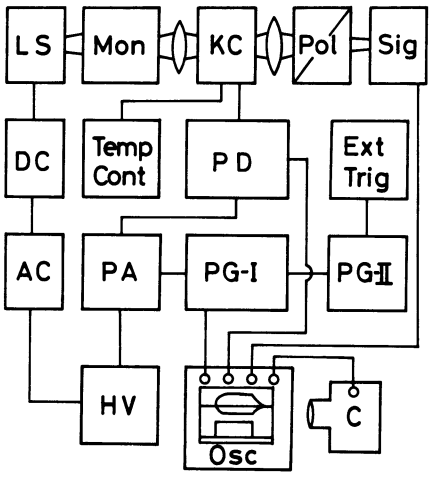

Fig. 1. Block diagram of pulsed linear electric dichroism apparatus. AC, Yamabishi Electric Co. NAC-1.5K voltage regulator; DC, Ewig & Co. HS-D200F starter-power supply; LS, light source; Mon, 25-cm tandem double monochromator; KC, "Kerr" cell and holder; Pol, magnesium fluoride polarizer; Sig, signal detector; HV, Kawaguchi Electric Works Model V-710 high-voltage DC power supply (0–10 kV); PA, homemade pulse amplifier; PD, pulse discharge network;[14] PG-I, Anritsu Electric Co. Model MG411B pulse generator; PG-II, Toyo Telesonic Co. Model 7103C pulse generator for baseline triggering; Ext Trig, homemade external trigger to activate the whole measuring system; C, Polaroid camera; Osc, 7844 dual beam oscilloscope; Temp Cont, regulated temperature bath.

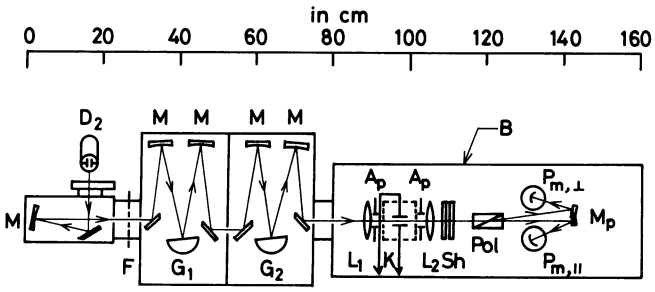

Fig. 2. Schematic diagram of optical system. D_2, deuterium lamp (see text); F, cut-off filter, M, concave mirror; G_1 and G_2, diffraction gratings; B, blackened aluminum enclosure; L_1 and L_2, quartz lenses; K, "Kerr" cell; A_p, rectangular aperture; Pol, polarizer; Sh, shutter; $P_{m,//}$ and $P_{m,\perp}$, photomultipliers; M_p, front-faced reflecting mirrors.

Spectroscopic Co. Model CT-25ND) is collimated by the first double-convex lens L_1 to the center of a "Kerr" cell K. The diverging beam is again converged onto the front of photomultipliers $P_{m,//}$ and $P_{m,\perp}$ by the second double-convex lens L_2. These lenses are made of strain-free far ultraviolet transmitting quartz (Extrasil grade), the focal length and the diameter being 55 mm and 33 mm respectively. A screen with a 4×10 mm rectangular aperture is placed behind L_1 and another with a 2×8 mm aperture is in front of L_2. A Rochon-type

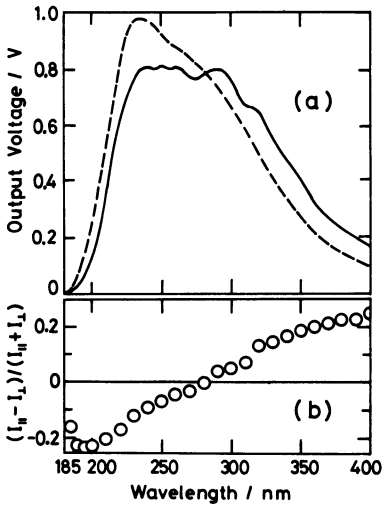

Fig. 3. The overall spectral intensity distribution of deuterium lamp in the ELD apparatus (a) and the wavelength dependence of the degree of polarization p (b). In (a), the light intensities, $I_{//}$ (——) and $I_\perp$ (----), were detected as the photomultiplier output voltage. In (b), $p=(I_{//}-I_\perp)/(I_{//}+I_\perp)$, where $I_{//}$ and $I_\perp$ are the intensities of light polarized parallel and perpendicular to the direction of electric field in the absence of a "Kerr" cell assembly.

magnesium fluoride beam-splitting polarizer Pol (MFR-9, Karl Lambrecht, Inc., Chicago, USA) is inserted. This prism is set in such a way that the emerging light is separated into two components; one, polarized parallel to the pulsed electric field, traveling straight and the other, polarized perpendicular to the field, traveling obliquely at an angle of 4.5° at 200 nm. Thus, both parallel- and perpendicularly-polarized emerging light beams can be detected *independently* and *simultaneously* without rotating the prism. Each of these beams is further separated and converged by placing a rectangular concave mirror M_p (11×42 mm) with a focal length of 60 mm, which reflects light from the front surface coated with aluminum and protected with magnesium fluoride.

The signal-detecting system consists of two matched side-on type R106UH photomultipliers (Hamamatsu TV Co.), each detecting the linearly polarized beam. The voltage generated by each P_m tube is led to either of the separate channels of the dual beam oscilloscope. Two signals and an attenuated pulse are all displayed simultaneously on a cathode-ray tube (CRT) and photographed with a Tektronix C-53 oscilloscope camera. Figure 3a shows the spectral characteristics of the photomultiplier output voltage with a 200 watt deuterium lamp in the 400—185 nm region. In the present optical system, the transmitted light intensity is both wavelength- and polarization-dependent. Figure 3b shows the degree of polarization for the overall optical system. In practice, however, these features do not interfere with the signal measurement at discrete wavelengths, since the instrument is operated manually.

A cylindrical high-voltage-resistant "Kerr" cell was made of either Kel-F or Acrylite plastics for the far ultraviolet region. The design of the cell is essentially

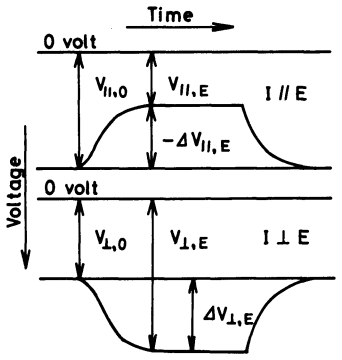

Fig. 4. Parallel- and perpendicular-polarized dichroism signals for data analysis. Notations are given in Eqs. 1–3 in text.

the same as the one described previously;[6,14] the gap between two highly polished electrode plates (stainless steel) is 0.327 cm and the optical path length is 0.60 cm. The volume of a sample solution is 0.2—0.3 ml. The Kerr cell is set inside the blackened brass block, through which a temperature-controlled fluid circulates with an accuracy of ±0.05 °C. The temperature of a sample is recorded with a small thermistor probe which is in direct contact wih the solution.

Data Analysis. Figure 4 schematically shows the dichroic signals displayed on a CRT screen. Let $I_{//,E}$ and $I_{//,0}$ be the parallel-polarized light intensities transmitting through the solution and the polarizer and falling onto a detecting tube in the presence and the absence of an external electric field. The difference in absorbances $\Delta A_{//}(=A^E_{//}-A)$ is given as[13,14]

$$\Delta A_{//} = \Delta\varepsilon_{//}Cl = (\varepsilon^E_{//}-\varepsilon)Cl = -\log\left(1+\frac{\Delta I_{//,E}}{I_{//,0}}\right) = -\log\left(1+\frac{\Delta V_{//,E}}{V_{//,0}}\right), \quad (1)$$

where C is the molar concentration of solute, l is the path length in cm, $\varepsilon^E_{//}$ and ε are the molar absorption coefficients of the solute, and $V_{//,E}$ and $V_{//,0}$ are the voltages generated across a load resistor in the presence and the absence of the external field. $\Delta V_{//,E}(=V_{//,E}-V_{//,0})$ should be determined within the range, in which the light intensity is linearly proportional to the voltage generated.[14] Similarly, for the perpendicularly-polarized light,

$$\Delta A_{\perp} = \Delta\varepsilon_{\perp}Cl = (\varepsilon^E_{\perp}-\varepsilon)Cl = -\log\left(1+\frac{\Delta I_{\perp,E}}{I_{\perp,0}}\right) = -\log\left(1+\frac{\Delta V_{\perp,E}}{V_{\perp,0}}\right). \quad (2)$$

The reduced dichroism is given from Eqs. 1 and 2 as

$$\frac{\Delta A}{A} = \frac{A^E_{//}-A^E_{\perp}}{A} = \frac{1}{A}\log\left(\frac{1+\dfrac{\Delta V_{\perp,E}}{V_{\perp,0}}}{1+\dfrac{\Delta V_{//,E}}{V_{//,0}}}\right). \quad (3)$$

If the applied electric pulse field orients solute molecules, but does not deform the molecular shape, then the following relation should hold:[15]

$$\frac{\Delta A_{//}}{A} = -\frac{2\Delta A_{\perp}}{A} \quad \text{and} \quad 3A = A^E_{//} + 2A^E_{\perp}. \quad (4)$$

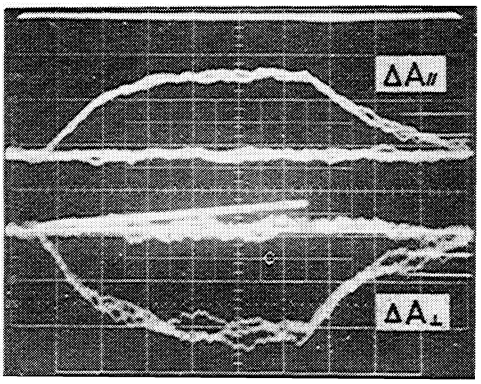

Fig. 5. Simultaneous display of transient dichroism signals for a collagen solution. Wavelength, 200 nm; field strength, 12.8 kV/cm; sweep timp, 100 μs/division.

Experimental

Materials and Measurements. Collagen (type III, acid soluble from calfskin) was purchased from Sigma Co. The sample was kindly purified by Dr. K. Gekko of Nagoya University by dissolving it in 0.5 M (1 M=1 mol dm^{-3}) acetic acid and centrifuging at 4 °C to remove precipitates. After repeating this procedure, the supernatant was dialyzed against distilled water and then freeze-dried. The collagen solution was prepared by dissolving the dried sample in 1 mM H_3PO_4 aqueous solution (pH=3.16), the concentration being 0.28 mM (=0.03 g dm^{-3}).[16,17] The isotropic spectrum was measured on a Hitachi EPS-3T spectrophotometer with a pair of 0.5 cm quartz cells. The electric dichroism was measured on the present apparatus with two Kerr cells; one (l=2.00 cm with a gap of 0.330 cm[14]) the 230—208 nm region and the other (l=0.60 cm with a gap of 0.327 cm) in the 206.5—187 nm region. The slit widths were adjusted manually, so that the half-intensity width was less than 2 nm at 200 nm. All measurements were performed at 20 °C under nitrogen gas purge (3 L/min).

Figure 5 shows an oscillogram of a collagen solution. Both $\Delta A_{//}$ and $\Delta A_{\perp}$ were traced three times to illustrate the reproducibility.

Results and Discussion

Dependence of Electric Dichroism on Field Strength. Figure 6 shows the dependence of the observed dichroism of collagen on the applied electric field at 200 nm. Parallel and perpendicular specific dichroic signals ($\Delta A_{//}/A$ and $\Delta A_{\perp}/A$) are plotted against the square of the field strength, E^2, together with the reduced dichroism ($\Delta A/A$) which was calculated with the aid of Eq. 3. The first relation in Eq. 4 holds up to 19 kV/cm, which indicates that no anomalous effect is induced by the applied field. The $\Delta A/A$ values tend to saturate at high fields. By extrapolating these values to infinitely high field, the saturated value, $(\Delta A/A)_s$, was estimated with due consideration for curvature.[18,19] This procedure is shown in Fig. 7, where $\Delta A/A$ values at 200 nm were plotted against E^{-1} and E^{-2} and the intercepts were determined to be 0.333 and 0.291 by linear least-square fitting. These values correspond to the upper and lower limits for the true value of $(\Delta A/A)_s$; the value of 0.333

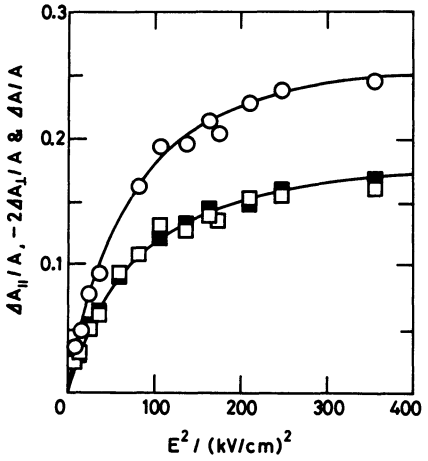

Fig. 6. Dependence of dichroism for a collagen solution on applied electric field. $\Delta A_{//}/A$ (□), $-2\Delta A_\perp/A$ (■), and $\Delta A/A$ (○) at 200 nm.

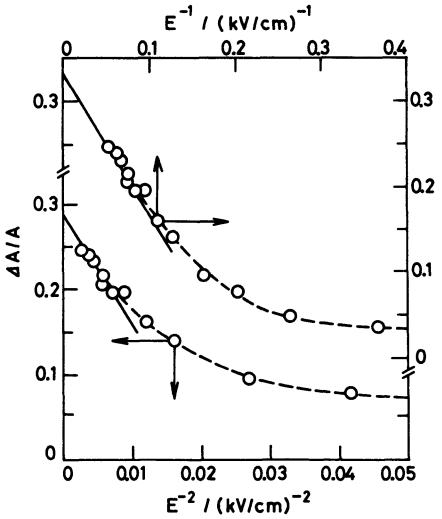

Fig. 7. Extrapolation of reduced dichroism to infinitely high field strength. The data were the same as those in Fig. 6. Solid lines represent the least-square fitting. Other details are given in text.

would be reached if the orientation of the collagen helices results from the pure permanent dipole moment, while the estimated value would be 0.291 if the orientation is solely due to the polarizability anisotropy.[18,19]

Dependence of Electric Dichroism on Wavelength. Figure 8 shows the dependence of dichroism on wavelength (upper half) and the anisotropic spectra, $A_{//}^E$ and $A_\perp^E$, at a constant field strength of 16.3 kV/cm, together with the isotropic spectrum of collagen, A, in the absence of the field (lower half). The reduced dichroism is positive but not constant throughout the 230—187 nm region, indicating that the broad single-peaked isotropic spectrum is only apparent and contains several transition moments directed at different angles relative to the orientation axis of a collagen molecule. These dichroic spectra of the peptide chromophore of collagen in solution could be determined, for the first time, with the present ELD apparatus. The $A_{//}^E$-spectrum with the maximum at 192 nm is always more

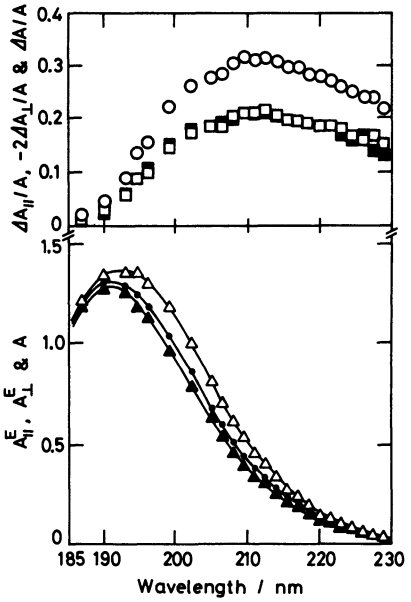

Fig. 8. The dependence of reduced dichroism on wavelength (upper half)and the anisotropic spectra (lower half) of collagen in an acid solution at 16.3 kV/cm. Upper half: $\Delta A_{//}/A$ (□), $-2\Delta A_\perp/A$ (■), and $\Delta A/A$ (○). Lower half: $A_{//}^E$ (-△-), $A_\perp^E$ (-▲-); the observed isotropic spectrum (——) and the isotropic absorbance calculated with $3A=A_{//}^E+2A_\perp^E$ (●). The path lengths are normalized to 0.60 cm in all cases.

intense than the $A_\perp^E$-spectrum with the maximum at 190 nm, both spectra coinciding with each other below 188 nm. It should be noted that these absorption maxima are shifted relative to the maximum of the isotropic spectrum at 191 nm. A similar trend was observed for a stroked collagen film.[20] Equation 4 holds over the entire wavelength region; the isotropic spectrum calculated with the relation, $3A=A_{//}^E+2A_\perp^E$, was indicated with dots (lower half).

Simulation of Reduced Dichroism. Collagen in a triple-stranded helix conformation is known to be oriented by a pulsed electric field, owing to the interaction predominantly with the permanent dipole moment borne on the polypeptide chains.[21-23] The orientation axis of collagen toward the electric field is the longitudinal axis of the triple helix. The degree of orientation (denoted as Φ) of collagen molecules in solution at a given orienting field strength of E is related to the reduced dichroism observed at E and the saturated dichroism as $\Delta A/A=(\Delta A/A)_s\times\Phi$,[15] Φ being independent of wavelength inasmuch as the value of E is specified. For example, $\Phi=0.72$ at $E=16.3$ kV/cm, since at 200 nm $\Delta A/A=0.240$ and $(\Delta A/A)_s=0.333$ (the last was estimated from the extrapolation of $\Delta A/A$ against E^{-1}). The value of $(\Delta A/A)_s$ may be calculated at any wavelength, once the value of Φ is known. It is related to the absorption transition moment by the following expression:[13]

$$\left(\frac{\Delta A}{A}\right)_s=\left(\frac{\Delta A}{A}\right)\left(\frac{1}{\Phi}\right)=\frac{3}{2}\frac{\sum_i(3\cos^2\theta_i-1)A_i}{\sum_i A_i}, \quad (5)$$

where θ_i is the angle between the transition dipole

moment direction of the ith absorption band with absorbance A_i and the orientation axis of a collagen molecule, *i. e.*, the long axis of the triple-stranded helix.

From the variation of $\Delta A/A$ with wavelength in Fig. 8, at least three overlapping component bands must be present in the peptide band; approximately the first is at 230—210 nm, the second at 210—200 nm, and the third at 200—185 nm. In order to simulate the wavelength dependence of $\Delta A/A$ with these bands, the isotropic spectrum must be decomposed into these three component bands. In this work, the profile of each band was assumed to be Gaussian as

$$A_i(\tilde{\nu}) = A_{i,\max}\exp\left[-(4\ln 2)\left(\frac{\tilde{\nu}-\tilde{\nu}_{i,\max}}{\delta_i(\tilde{\nu})}\right)^2\right], \quad (6)$$

where $A_i(\tilde{\nu})$ is the absorbance at a given wave number $\tilde{\nu}$, $A_{i,\max}$ is the maximum absorbance at the peak position $\tilde{\nu}_{i,\max}$, and $\delta_i(\tilde{\nu})$ is the half-intensity band width where $A_i/A_{i,\max}=0.5$.

Figure 9 shows a decomposition of the observed isotropic spectrum (circles) into three component bands (dashed lines) centered at 219 nm, 200 nm, and 189 nm. The resultant spectrum (solid line), composed of these three bands, is in excellent agreement with the observed spectrum. With the characteristic parameters for $A_{i,\max}$ (i=1—3) given in Table 1, the experimentally obtained values of $\Delta A/A$ were fitted by adjusting the angle θ_i with the aid of Eq. 5. The best values of θ_i (i=1—3) are given in Table 1. The agreement between the experimental and simulated values of $\Delta A/A$ is good throughout the 230—187 nm region. Since collagen is a complex protein consisting of many different amino acid residues, it would not be relevant further to refine the simulated wavelength dependence of $\Delta A/A$ values by decomposing the isotropic spectrum into four or more component bands.

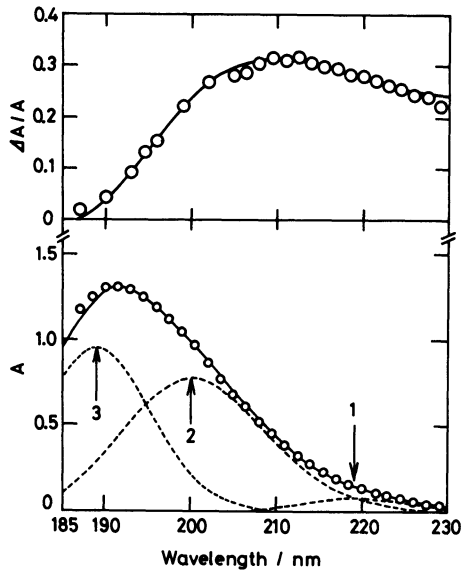

Fig. 9. Decomposition and simulation of the isotropic spectrum and the wavelength dependence of $\Delta A/A$ of collagen. Upper half: observed values of $\Delta A/A$ (○) and the simulated dependence of $\Delta A/A$ (——) on wavelength. Lower half: observed (○) and simulated (——) isotropic spectra, together with three component bands (----). These are: (1) the 219 nm band, (2) the 200 nm band, and (3) the 189 nm band. The experimental data are taken from Fig. 8.

The Peptide Chromophore in Collagen. There have been two reports, one by Mandel and Holzwarth[20] and the other by Jenness *et al.*,[17] in which the optical properties of collagen were quantitatively studied in solutions and in stroked films. These workers, however, failed to identify the first component band at 219 nm that was detected in this work. This transition may be assigned to the n-π^* transition on the carbonyl oxygen because of its weak intensity and long wavelength peak.[17,20] It is the wavelength dependence of the reduced dichroism, but not of the dichroism, $\Delta A_{/\!/}$ or $\Delta A_{\perp}$,[20] itself that reveals the hidden features in an isotropic spectrum, such as the number of transition moments and the angles, in a tangible fashion. Since Eq. 5 yields only the absolute magnitude for the angle θ_i, it may be said that the direction of the n-π^* transition makes an angle +(50.6—51.0°) or −(50.6—51.0°) (θ_1) with respect to the orientation axis of a collagen molecule.

The second component band at 200 nm is associated with a positive dichroism with an angle +(48.8—49.5°) or −(48.8—49.5°) (θ_2), while the third band at 189 nm is associated with a negative dichroism with an angle of +(56.0—55.8°) or −(56.0—55.8°) (θ_3). The presence of these bands has been noted both in the isotropic spectrum and in the anisotropic spectra of collagen films.[20] On the basis of Moffitt's prediction,[24] Mandel and Holzwarth have assigned these bands to the exciton-split π-π^* transitions which are expected for a single-stranded helix.[20,24] The allowed exciton bands are polarized parallel and perpendicular to the axis of the helix. According to the prediction, the positive 200-nm band is the parallel (//) band, while the negative 189-nm band is the perpendicular (⊥) band. As mentioned above, the wavelength dependence of $\Delta A/A$ can afford the angle relative to the orientation axis which is the axis of the triple-stranded helix of collagen. The estimated angles are about ±49°, but not 0°, for the "//-band" and about ±56°, but not 90°, for the "⊥-band". This discrepancy between the observed and theoretically expected values for angles θ_2 and θ_3 may be

Table 1. The optical property of collagen in acid solution

i	$\tilde{\nu}_{i,\max}\times 10^{-4}$ / cm^{-1}	$A_{i,\max}$	$\delta_i\times 10^{-4}$ / cm^{-1}	$\lvert\theta_i\rvert$ / deg
1	4.57 (219)[a]	0.07	0.33	50.6[b] (51.0)[c]
2	5.00 (200)[a]	0.77	0.48	48.8[b] (49.5)[c]
3	5.29 (189)[a]	0.95	0.40	56.0[b] (55.8)[c]

a) Values in parentheses are the peak positions expressed with wavelength in nm. b) Angles calculated from $(\Delta A/A)_s$ which were obtained by the E^{-1} extrapolation. c) The same obtained by the E^{-2} extrapolation.

attributed to three possibilities which remain to be resolved.

The first possibility is that the exciton band is not formed over the collagen helix which consists of three intermolecular hydrogen-bonded helix chains. The second is that the exciton splitting does occur, but it is limited only to each single-stranded helix chain which is coiled around the collagen axis. The third is that the Moffitt-type splitting does not actually occur, and the observed component bands all belong to the intrinsic peptide chromophore. These are interesting poins for future investigations, which must be deferred until the geometry of the collagen helix and the optical property of small-molecular-weight amide compounds are more thoroughly clarified.

Conclusion

We have constructed a high-voltage pulsed electric linear dichroism apparatus with the aim of unraveling the optical properties of the chromophores involved in biologically important macromolecules, which absorb light in the far ultraviolet region. Using this apparatus, we have measured the dichroic spectra of collagen in an acid solution over the 230—187 nm region, in which the reduced dichroism was found to be wavelength-dependent. We have presented a detailed, analytical procedure for electric dichroism data. On the basis of this analysis, we concluded that the isotropic absorption spectrum of collagen contains at least three transition moments, which make different angles with respect to the orientation axis of the collagen helix.

We are deeply indebted to Dr. E. Charney of the National Institutes of Health (Bethesda, Md., USA) for kindly lending us a magnesium fluoride polarizer in the initial stage of this work. This work was in part supported by a Grant-in-Aid for Scientific Research (No. 347009) from the Ministry of Education, Science, and Culture.

References

1) E. Fredericq and C. Houssier, "Electric Dichroism and Electric Birefringence," Clarendon Press, Oxford (1973).
2) K. Yamaoka, "Polyelectrolytes" (in Japanese), vol. 13, "Kobunshi Jikkengaku," ed by M. Kaneko, S. Sugai, and M. Nagasawa, Kyoritsu Press, Tokyo (1978), Chap. 9. pp. 230—255.
3) C. M. Paulson, Jr., "Molecular Electro-Optics," Part 1, ed by C. T. O'Konski, Marcel Dekker, New York (1976), Chap. 7, pp. 243—273.
4) K. Yoshioka, "Molecular Electro-Optics," Part 2, ed by C. T. O'Konski, Marcel Dekker, New York (1978), Chap. 17, pp. 601—643.
5) M. Shirai, "Molecular Electro-Optics," Part 2, ed by C. T. O'Konski, Marcel Dekker, New York (1978), Chap. 19, pp. 685—711.
6) K. Yamaoka and E. Charney, *Macromolecules*, **6**, 66 (1973).
7) J. Bontemps, C. Houssier, and E. Fredericq, *Biophys. Chem.*, **2**, 301 (1974).
8) C. Houssier, B. Hardy, and E. Fredericq, *Biopolymers*, **13**, 1141 (1974).
9) M. Tricot, C. Houssier, and V. Desreux, *Biophys. Chem.*, **3**, 291 (1975).
10) N. E. Geacintov, A. Gagliano, V. Ivanovic, and I. B. Weinstein, *Biochemistry*, **17**, 5256 (1978).
11) H. H. Chen and E. Charney, *Biopolymers*, **19**, 2123 (1980).
12) K. Yamaoka and K. Matsuda, *Macromolecules*, **14**, 595 (1981).
13) K. Matsuda and K. Yamaoka, *Bull. Chem. Soc. Jpn.*, **55**, 69 (1982).
14) K. Yamaoka and K. Matsuda, *J. Sci. Hiroshima Univ. Ser. A*, **43**, 185 (1980).
15) K. Yamaoka and E. Charney, *J. Am. Chem. Soc.*, **94**, 8963 (1972).
16) W. B. Gratzer, W. Rhodes, and G. D. Fasman, *Biopolymers*, **1**, 319 (1963).
17) D. D. Jenness, C. Sprecher, and W. C. Johnson, Jr., *Biopolymers*, **15**, 513 (1976).
18) E. Charnery and K. Yamaoka, *Biochemistry*, **21**, 834 (1982).
19) K. Yamaoka and K. Fukudome, *Bull. Chem. Soc. Jpn.*, **56**, 60 (1983).
20) R. Mandel and G. Holzwarth, *Biopolymers*, **12**, 655 (1973).
21) K. Yoshioka and C. T. O'Konski, *Biopolymers*, **4**, 499 (1966).
22) J. C. Bernengo, B. Roux, and D. Herbage, *Biopolymers*, **13**, 641 (1974).
23) S. Umemura, M. Sakamoto, R. Hayakawa, and Y. Wada, *Biopolymers*, **18**, 25 (1979).
24) W. Moffitt, *Proc. Natl. Acad. Sci. U.S.A.*, **42**, 736 (1956).